OPTOELECTRONICS AND ADVANCED MATERIALS – RAPID COMMUNICATIONS Vol. 3, No. 6, June 2009, p. 569 - 573

Temperature-dependent scattering processes of n-type indium antimonide

K. ALFARAMAWI*, M. A. ALZAMIL
Physics Department, Teachers College, King Saud University, Riyadh, Saudi Arabia

Calculations of the electron mobility of n-type InSb have been performed at different temperature regimes using relaxation time approximation method. The temperatures were classified into three main categories according to the electron mobility behavior. A high temperature range was considered from room temperature down to approximately 100 K. Intermediate temperature range was taken from 100 K down to 50 K. The low range was assumed from 50 K down to 10 K. In these temperature ranges a number of scattering sources have been discussed. Neutral impurity scattering, ionized impurity scattering and lattice scattering were analyzed. At high temperature regime, the intrinsic behavior of n-doped InSb was noticed. At intermediate temperature range the lattice scattering was recorded as the dominant scattering center. The ionized impurity scattering was thought to be the major one at low temperature region. Comparison with experimental results was also mentioned.

(Received April 30, 2009; accepted June 15, 2009)

Keywords: Narrow band gap, Mobility, Impurity scattering, Lattice scattering

1. Introduction

At present, III–V compound semiconductors provide the materials basis for a number of well-established commercial technologies, as well as new cutting-edge classes of electronic and optoelectronic devices. Few examples include high-electron-mobility and heterostructure bipolar transistors, diode lasers, light-emitting diodes, photodetectors, electro-optic modulators and frequency-mixing components [1].

InSb is a direct semiconductor, the minimum of the conduction band is situated in the center of the Brillouin zone. Near the minimum, the energy is isotropic but non-parabolic [2]. For values of wave vector far from the conduction band minima, the energy deviates from the simple quadratic expressions and nonparabolcity occurs.

InSb is the III–V binary semiconductor having the smallest band gap with high carrier mobility and small effective mass. For many years it has been a touchstone for band structure computational methods [3,4]. Numerous studies of the fundamental transport properties and their temperature dependences have been conducted over the last three decades [5-9].

The scattering mechanisms, which govern the electron mobility in InSb, are; ionized impurity scattering (significant at low temperatures), neutral impurity scattering, acoustic phonon deformation mode, piezoelectric acoustic mode and optical phonon scattering.

In the present study, a theoretical investigation of some electrical transport properties is realized. Calculations of the electron mobility have been performed at different temperature regimes using relaxation time approximation method.

2. Theory

The electrom mobility considering various scattering mechanisms can be given by solving Boltzmann equation in the relaxation time approximation as

$$\mu = \frac{e\langle\tau\rangle}{m^*} \tag{1}$$

where μ is the mobility, $\langle\tau\rangle$ is the average relaxation time over the electron energies, e is the electronic charge and m^* is the effective mass of the electron. In what follows, the expressions of relaxation time and mobility due to different scattering mechanisms will be presented.

2.1 Ionized impurity scattering

The strength of scattering due to electrostatic forces between the carrier and the ionized impurity centers depends on the interaction time and the number of impurities. Larger impurity concentrations result in a lower mobility [10,11]. The formula for calculating the average relaxation time is given by [11]:

$$\langle\tau_{ii}(\varepsilon)\rangle = \frac{e}{m^*}\frac{\int_0^\infty \tau_{ii}(\varepsilon)\,\varepsilon^{3/2}\,\frac{df_o}{d\varepsilon}\,d\varepsilon}{\int_0^\infty \varepsilon^{3/2}\,\frac{df_o}{d\varepsilon}\,d\varepsilon} \tag{2}$$

where ε is the energy and f_o is the electrons distribution function. The mobility associated with the ionized

impurity scattering (μ_{ii}) has been calculated as a function of the temperature *(T)* as:

$$\mu_{ii} = \frac{A}{B} T^{3/2} \tag{3}$$

where

$$A = \frac{128\sqrt{2}\,\pi^{1/2} \in^2 k^{3/2}}{N_i e^3 m^{*1/2}} \tag{3a}$$

$$B = \ln(1+y) - \frac{y}{1+y} \tag{3b}$$

$$y = \frac{24 \in m^* k^2}{\hbar^2 e^2 n} T^2 \tag{3c}$$

Here $\in$ is the dielectric constant of the host material, k is Boltzmann constant, N_i is the concentration of the ionized impurities, $\hbar$ is Planck' s constant and n is the concentration of the carriers.

2.2 Neutral impurity scattering

When an electron passes close to neutral atom, momentum can be transferred through a process in which the free electron exchanges with a bound electron on the atom. The relaxation time can be written as [12]

$$\tau_{ni}(\varepsilon) = \frac{m^*}{20\, N_n \hbar\, a_B}$$

where N_n is the concentration of the neutral impurities and a_B is the effective Bohr radius. The mobility due to neutral impurity scattering is then given by

$$\mu_{ni} = \frac{e^3 m^*}{80\pi\, N_n \in \hbar^3} \tag{4}$$

The neutral impurity scattering process is a temperature independent and then the mobility associated to it is expected to be a constant through the material under consideration.

2.3 Acoustic phonon: deformation potential scattering

The acoustic mode lattice vibration induced changes in lattice spacing, which change the band gap from point to point. Since the crystal is "deformed" at these points, the potential associated is called the deformation potential. The corresponding relaxation time can be written as [13]

$$\tau_{dp}(\varepsilon) = \frac{\pi \hbar^4 \rho s^2}{\sqrt{2}\, E_1^2\, m^{*3/2} (kT)} \varepsilon^{-3/2}$$

where ρ is the crystal mass density, s is the average velocity of sound and E_1 is the deformation potential. Here $\rho s^2 = c_1$ is the longitudinal elastic constant. The mobility associated with the deformation potential scattering is given by

$$\mu_{dp} = \frac{C}{T^{3/2}} \tag{5}$$

where

$$C = \frac{2\sqrt{2}\pi^{1/2}\hbar^4 \rho s^2 e}{3E_1^2\, m^{*5/2}\, k^{3/2}} \tag{5a}$$

2.4 Acoustic phonon: piezoelectric potential scattering

Electrons can suffer scattering with piezoelectric mode of acoustic lattice vibrations. In this scattering mechanism, the energy change during the collisions is small. The relaxation time due to piezoelectric potential scattering is

$$\tau_{pe}(\varepsilon) = \frac{2\sqrt{2}\pi \hbar^2 \in}{e^2 P^2 m^{*1/2} (kT)} \varepsilon^{1/2}$$

where $P = \left(\frac{p_e^2}{\rho s^2 \in}\right)$ is the piezoelectric coupling coefficient and p_e is the piezoelectric constant. The mobility as a result of piezoelectric potential scattering is given by

$$\mu_{pe} = \frac{D}{P^2 T^{1/2}} \tag{6}$$

and

$$D = \frac{16\sqrt{2}\pi^{1/2} \in \hbar^2}{3e\, m^{*3/2}\, k^{1/2}} \tag{6a}$$

It was reported that at 300 K, the piezoelectric potential scattering rate is about five times smaller than the deformation potential rate [14].

3. Calculated results and discussion

The temperature variation of the band gap of InSb is first studied in the temperature range from room temperature down to 10 K. The equation used in this study is of the form [15]

$$E_g(T) = E_g(0) - \left[\frac{\alpha T^2}{\theta + T}\right] \tag{7}$$

The parameters $\alpha = 3.2 \times 10^{-4}$ *eV/K* and $\theta = 220$ *K* were used in the calculations [15]. Fig. 1 shows the

calculated energy gap variation with temperature down to 10 K. It is noticed from the figure that the gap at room temperature is 0.179 eV. This means that electrons from host material will be found in the conduction band at room temperature due to the thermal excitation while most of donors will be ionized because of the very small donor activation energy of such system (of order of 10^{-3} eV [16]). By lowering down the temperature, both carrier concentration and mobility will change and then transport properties will depend on the range of temperature of interest. According to the published experimental work of n-InSb system [17], we will divide the temperatures into three regions: high, intermediate and low temperature ranges.

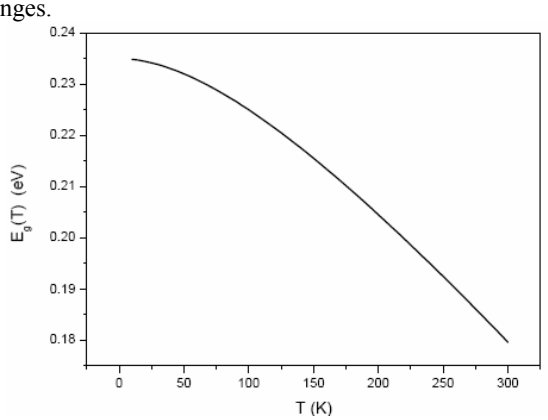

Fig. 1. Energy gap variation with temperature.

3.1 High temperature range

This region extends from room temperature down to 100 K. At sufficient high temperatures (around 300 K and above), the characteristics of InSb material is considered to be due to the intrinsic charge carriers. It is then appropriate to calculate the intrinsic carrier density and the drift mobility at this temperature range. The mobility of the electrons in InSb around room temperature could be estimated from the relation [18]

$$\mu_{in} = 7.7 \times 10^4 \left(\frac{T}{300} \right)^{-5/3} \qquad cm^2 / V.s \quad (8)$$

The intrinsic carrier concentration in InSb was presented by Gunningham and Gruber [18] from the expression

$$n_{in} = 5.76 \times 10^{14} T^{3/2} \exp\left(\frac{-0.129}{kT} \right) \qquad cm^{-3} \quad (9)$$

Fig. 2 demonstrates the simulation of the mobility with the inverse of temperature in this regime, inset is the carrier concentration.

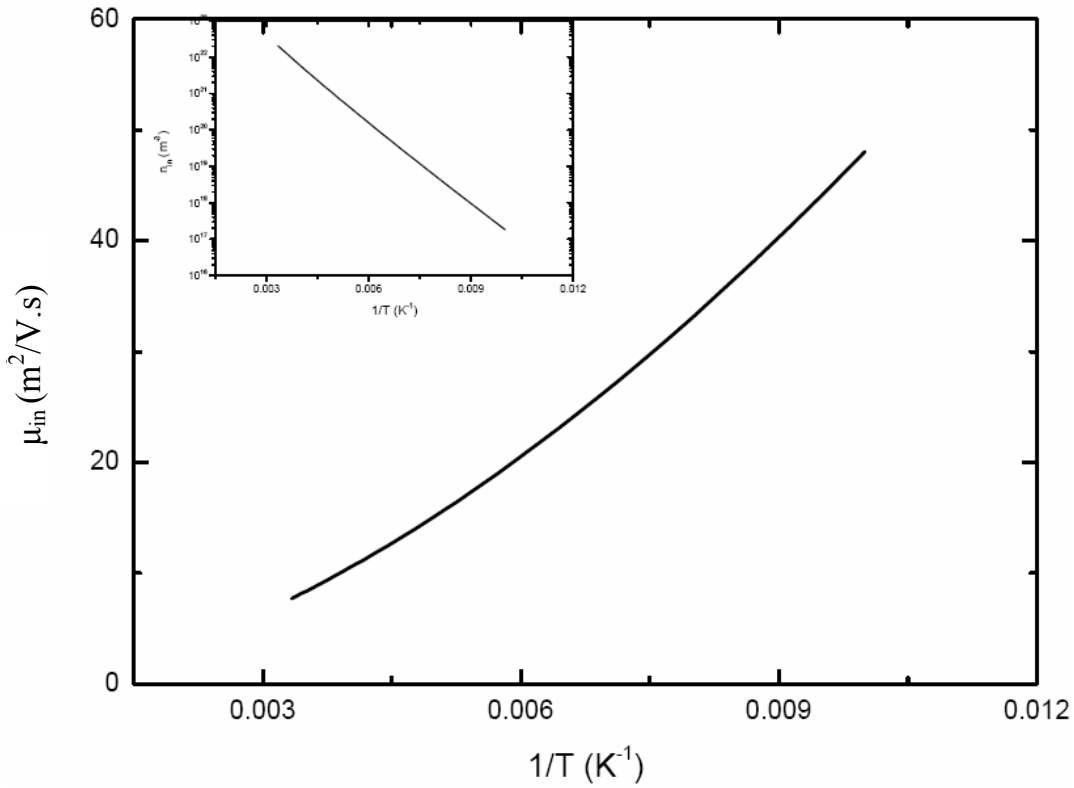

Fig.2. Intrinsic mobility versus temperature; inset is the carrier concentration.

The electron mobility increases by lowering the temperature while the electron concentration decreases. The increase in the mobility in this regime may be attributed mainly to the sharp decrease in the electron density in the conduction band.

3.2 Intermediate temperature range

The range of temperature here is from 100 K to 50 K. As the thermal energy becomes small, the main contribution to the mobility is due to the extrinsic carriers. It was mentioned that the dominant scattering centers at this range is the acoustic phonons with the two modes: deformation potential and piezoelectric [19]. The calculated results for mobilities including acoustic phonons through potential deformation and piezoelectric at different temperatures have been presented using the parameters of n-type InSb shown in Table 1.

Table 1. Material parameters.

Parameter	Value	Reference
Effective mass (m^*)	0.014 m_o	[2]
Static dielectric constant ($\in$)	17.9	[2]
Energy gap (E_g) at 0 K	0.235 eV	[9]
Mass density (ρ)	5.79×10^5 g/cm^3	[1]
Velocity of sound (s)	1.8×10^5 cm/s	[1]
Acoustic deformation potential (E_1)	30 eV	[2]
Piezoelectric coefficient (p_e)	0.027	[9]

Fig. 3 represents the mobility versus temperature in case of deformation potential and piezoelectric scattering. Scattering with the two modes produces elevation in the mobility by decreasing of temperature.

The mobility due to piezoelectric acoustic phonon scattering is much greater than that of deformation potential. The combined mobility is now simply given by Matthiessen's rule:

$$\mu_{ac}^{-1} = \mu_{dp}^{-1} + \mu_{pe}^{-1} \qquad (10)$$

Fig. 3 shows the resultant mobility due to acoustic phonons, it is very close to the values of deformation potential scattering. This lets one to ignore the scattering due to piezoelectric potential especially at higher temperatures.

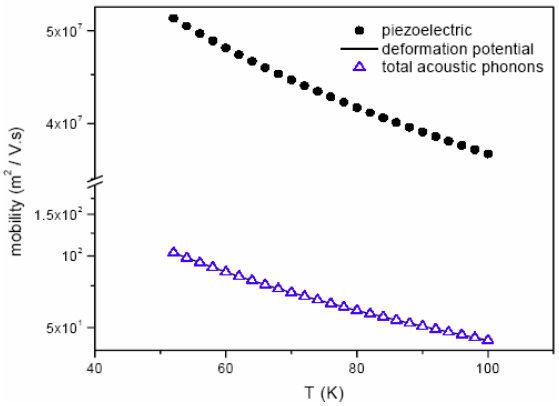

Fig. 3. Mobility versus temperature corresponding to acoustic phonon scattering.

3.3 Low temperature range

This region is supposed to extend from 50 K down to 10 K. Since the number of phonons in this range of temperature is much smaller than the ones in the previous higher range, the dominant scattering process in this regime is taken to be by ionized impurities. Fig. 4 shows the calculated mobility versus temperature corresponding to ionized impurity scattering for three concentrations of electrons. The value of the ionized impurity concentration corresponds to each carrier concentration is shown in table 2 [20]. The parameters used in the calculation are listed in Table 1.

Table 2. Electron concentrations and corresponding impurity concentrations [20].

Electron concentration	Ionized impurity concentration
$n = 9.5 \times 10^{19}$ m^{-3}	$N_i = 4.7 \times 10^{20}$ m^{-3}
$n = 1.44 \times 10^{20}$ m^{-3}	$N_i = 5.3 \times 10^{20}$ m^{-3}
$n = 3.4 \times 10^{20}$ m^{-3}	$N_i = 7.56 \times 10^{20}$ m^{-3}

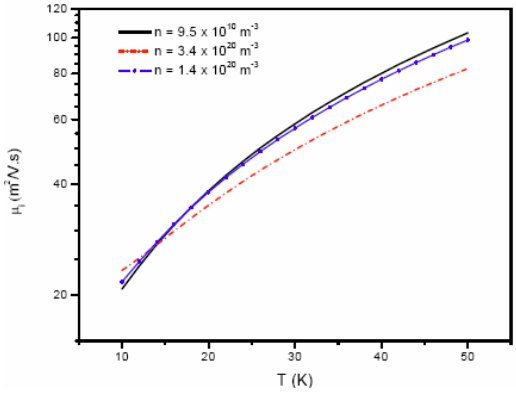

Fig. 4 Mobility versus temperature corresponding to ionized impurity scattering.

The effect of the neutral impurity scattering on the mobility is also considered. For the case of $n = 9.5 \times 10^{19}\ m^{-3}$, the density of neutral impurities is $N_n = 3.75 \times 10^{20}\ m^{-3}$. Using these data and the parameters in Table 1 one can obtain the value of the mobility due to neutral impurities as $\mu_{ni} = 3.22 \times 10^4\ cm^2/V.s$.

Fig. 5 demonstrates the overall mobility variation at the three ranges of temperatures. The figure matches well with the previously published experimental data on such system [17].

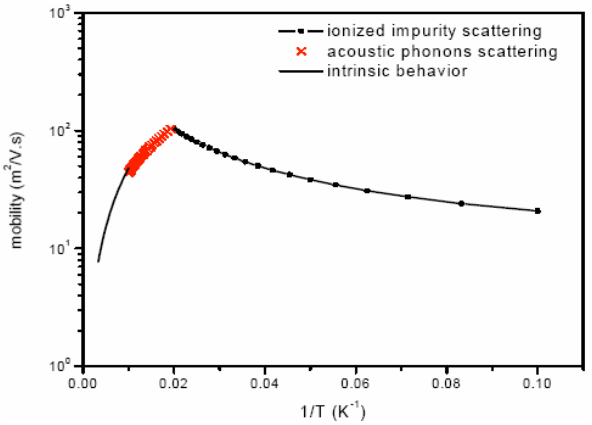

Fig. 5. Mobility behavior at all temperature ranges.

4. Conclusions

Numerical calculations of the electron mobility as a function of temperature have been carried out for n-type InSb semiconductor. Band gap variation with temperature was also analyzed. The calculations produced a value of 0.179 eV for the energy gap at room temperature. At temperatures from room to 100 K the intrinsic behavior of the crystal was considered. Both mobility and carrier concentration were identified. At temperatures from 100 K to 50 K the acoustic lattice vibrations with the two modes: deformation potential and piezoelectric potential were assumed to represent the dominant scattering centers for the electrons. The theoretical investigations have shown that the piezoelectric mode of scattering is negligibly small especially at higher temperatures. At low temperatures, below 50 K, the ionized impurity scattering limits the electron mobility. The overall mobility through the whole temperature range showed a good agreement with the previously published experimental data on this system.

5. References

[1] I. Vurgaftman, J. R. Meyer, L. R. Ram-Mohan, J. Appl. Phys. **89**, 11(2001).
[2] O. Ozbas, M. Akarsu, Turk. J. Phys. **26**, 283(2002).
[3] E. O. Kane, J. Phys. Chem. Solids **1**, 249 (1957).
[4] M. Razeghi, Opto-Electron. Rev. **6**, 155 (1998).
[5] Landolt-Bornstein, Numerical Data and Functional Relationships in Science and Technology, edited by O. Madelung, M. Schultz, and H. Weiss, New series, **17**, 1982; reprinted in O. Madelung, editor, Semiconductors-Basic Data, 2nd ed., Springer, New York, 1996.
[6] H. C. Casey, Jr., M. B. Panish, Heterostructure Lasers, Part A: FundamentalPrinciples, Academic, New York, 1978.
[7] Handbook Series on Semiconductor Parameters, edited by M. Levinshtein, S. Rumyantsev, M. Shur, World Scientific, Singapore, **1-2**, 1996.
[8] Z. M. Fang, K. Y. Ma, D. H. Jaw, R. M. Cohen, G. B. Stringfellow, J. Appl. Phys. **67**, 7034 (1990).
[9] Y. J. Jung, M. K. Park, S. I. Tae, K. H. Lee, H. J. Lee, J. Appl. Phys. **69**, 3109 (1991).
[10] S. Dhar, S. Ghosh, J. Appl., Phys. **96**, 5(1999).
[11] S. Mallick, J. Kundu, C. K. Sarkar., Can. J. Phys. **86**, 8(2008).
[12] J. Kundu, C. K. Sarkar, P. S. Mallick, Semicond. Phys., Quantum Elect. & Optoelect., **10**, 1 (2007).
[13] D. A. Anderson, N. Apsley, Semicond. Sci. and Techn. **1**(6), 9 (1986).
[14] D. C. Look, Electrical Characterization of GaAs materials and Devices, Wiley, New York, 1989.
[15] Y. J. Jung, M. K. Park, S. I. Tae, K. H. Lee, H. J. Lee, J. Appl. Phys. **69**, 5 (1991).
[16] S. Abboudy, R. Mansfield, P. Fozooni, Solid State Physics **71**, 518 (1987).
[17] K. Alfaramawi, S. Abboudy, L. Abulnasr, Int. J. Pure and Appl. Phys. **3**, 1 (2007).
[18] L. I. Berger, Semiconductor Materials, CRC Press, Boca Raton, FL, 1997.
[19] R. A. Smith, Semiconductors, Cambridge University press, 1959.
[20] S. S. Murzin, P. V. Popov, JETP Lett. **58**, 4 (1993).

*Corresponding author: kalfaramawi@yahoo.com